PPPL--1913

DE82 018138

MODELS FOR POLOIDAL DIVERTORS*

D. E. Post, D. Heifetz, and M. Petravic

Plasma Physics Laboratory, Princeton University

Princeton, New Jersey 08544

ABSTRACT

Recent progress in models for poloidal divertors has both helped to explain current divertor experiments and contributed significantly to design efforts for future large tokamak (INTOR, etc.) divertor systems. These models range in sophistication from zero-dimensional treatments and dimensional analysis to two-dimensional models for plasma and neutral particle transport which include a wide variety of atomic and molecular processes as well as detailed treatments of the plasma-wall interaction. This paper presents a brief review of some of these models, describing the physics and approximations involved in each model. We discuss the wide variety of physics necessary for a comprehensive description of poloidal divertors. To illustrate the progress in models for poloidal divertors, we discuss some of our recent work as typical examples of the kinds of calculations being done.

*Presented at the Fifth International Conference on Plasma Surface Interactions, Gatlinburg, Tennessee, May 3-7, 1982.

TABLE OF CONTENTS

I. INTRODUCTION

Divertors have long been proposed and tried for impurity control and pumping of tokamaks and stellarators [1-3]. The operation of a divertor is simple in concept. The plasma is diverted from the plasma edge by a coil which carries a current parallel to the plasma current (Fig. 1). At a null point between the coil and the plasma center, the poloidal field is zero. Plasma outside of this null point flows in the flux surface that encircles both the coil and the main plasma and can thus be diverted away from the main plasma.

In the divertor chamber (Fig. 2), the plasma flows along the field lines until it strikes the neutralizer plate. The ions and electrons recombine on the plate and are emitted from the plate as neutral atoms or molecules. These neutral particles then travel back down the divertor channel or pumping system, colliding with the walls and the plasma. Although previous reactor designs had considered poloidal divertors [4,5], the recent INTOR studies have helped focus attention on them [6].

A large fusion experiment such as INTOR will have a fusion yield of 500 megawatts and contain roughly 2×10^{22} particles with a particle confinement of roughly 0.1-1 seconds. It will thus produce a thermal flux to the first wall and divertor or limiter of 100 megawatts. This heat must be removed from the system without causing serious impurity problems in the plasma, or causing excessive erosion of the first wall and other material structures exposed to the plasma. Five-hundred megawatts of fusion yield implies a helium production of 2×10^{20} atoms/sec which has to be removed if the experiment is to last longer than a few seconds. The removal of this helium ash has to be accomplished with reasonably sized pumping systems and with minimum pumping of tritium.

Using simple sheath theory [7], we can make naive estimates of the edge plasma parameters which indicate the nature of these problems and their implications for the design of large fusion experiments. Assuming the edge plasma is transparent to neutrals and that all of the particles and heat are exhausted along field lines into a limiter or divertor, the heat flux Q, and particle flux Γ at the edge can be written as $Q \approx 8nv_F TA$, $\Gamma \sim nv_F A$, where v_F is the flow velocity ($\sim \sqrt{T/M}\sin\alpha$ where α is the shallow angle the field lines make with the neutralizing surface, T is the temperature, and M is the ion mass), n is the electron density, the factor eight comes from assuming no secondary electron emission and equal ion and electron temperatures, and A is the collecting area. Assuming a toroidal collecting limiter or divertor with a 30 cm width (ℓ) and a plasma major radius of 500 cm, $A = 2\pi R\ell \sim 10^5 cm^2$. These conditions yield an edge temperature of $T = (Q/8\Gamma)$. Writing $\Gamma = N/\tau$, where N is the number of particles in the discharge (2×10^{22} for INTOR) and τ is the overall particle confinement time, we have $T = Q\tau/8N \sim 4000$ eV $\times\ \tau$. For a τ of 200 milliseconds, $T \sim 800$ eV, and $n = 4 \times 10^{11} cm^{-3}$. The erosion rates associated with these edge conditions (a sheath potential of ~ 2.5 keV) are large, 11 cm/year for iron neutralizer plates. In addition, simple considerations of the pumping speed required to exhaust the helium (which might be allowed to build up to $\sim 5\%$ of the plasma density) indicates that massive pumping systems of the order of $10^7 \ell$/sec would be needed.

The difficulty of designing $10^7 \ell$/sec pumping systems and of finding materials with sputtering yields in the 10^{-8} to 10^{-4} range provides an enormous incentive to try to change the plasma edge conditions so that the particle energies in the divertor chamber are below the sputtering thresholds of normal materials and reasonably sized pumping systems in the $10^5 \ell$/sec range can be used. This has led to attempts to model the plasma and neutral transport in divertors and near limiters to explore ways to produce a cooler, denser edge.

II. OVERVIEW OF PHYSICS

A reasonable model for transport in the plasma edge involves a large number of diverse physical processes (Fig. 3). The basic picture is that ions and electrons flow out both across the flux surfaces as well as along the field lines. The ions and electrons recombine largely at a neutralizer plate or limiter and re-enter the plasma as neutrals. The neutral atoms and molecules transport through the plasma reflecting from the walls and undergoing charge exchange and ionizing collisions. Impurities are produced from the walls by sputtering, arcing, vaporization, chemical erosion, desorption, etc. The first requirement is for a set of equations to describe the transport of the edge plasma both along the field lines and normal to them.

Zero-dimensional, one-dimensional, and two-dimensional models have been constructed. The zero-dimensional models [9-11] include a wide variety of atomic and molecular processes and have been used for plasma breakdown calculations as well. The equations are of the form of

$$\frac{\partial f}{\partial t} = S - \frac{f}{\tau_{\parallel}} - \frac{f}{\tau_{\perp}} , \tag{1}$$

where f is either a particle or energy density in the edge, S is a source term, such as ionization, recombination, or charge exchange, $\tau_{\parallel}$ is a parallel loss time, and $\tau_{\perp}$ is a perpendicular loss time. Such models have been useful because of their simplicity and because one can easily include a wide variety of processes. They have been especially useful in modeling ion sources for neutral beams [12] and tokamak start up [9,10].

The next level of sophistication involves a generalization to replace the perpendicular part of Eq. (1) with a one-dimensional equation for the perpendicular transport. This is usually done [13-15] in the context of a conventional one-dimensional tokamak transport code [16,17], where the transport equations are of the form

$$\frac{\partial n}{\partial t} = \nabla_\perp \cdot \Gamma_\perp + S_n - \frac{n}{\tau_n} , \tag{2}$$

$$\frac{\partial \varepsilon}{\partial t} = \nabla_\perp \cdot Q_\perp + S_\varepsilon - \frac{\varepsilon}{\tau_\varepsilon} ,$$

where n and ε are the plasma and plasma energy densities, $\Gamma_\perp$ and $Q_\perp$ are the perpendicular particle and energy fluxes, S_n and S_ε are the respective sources, and τ_n and τ_ε are the respective parallel loss terms. The parallel loss terms are used only on those field lines that intersect a limiter or divertor. Steady-state analytic models of this form have also been constructed [18,19].

These models and variants of them have been useful in defining the expected conditions of a limiter scrapeoff or diverted edge plasma. They form a natural set of boundary conditions at the edge for one-dimensional transport codes. Applying these models to examine the expected edge conditions for INTOR produces estimates of $T_i \sim 100\text{-}200$ eV, $T_e \sim 100\text{-}300$ eV, and $n_e \sim 2 \times 10^{12}$ to $10^{13} \mathrm{cm}^{-3}$ (Fig. 4).

An alternate approach to one-dimensional models has been to replace the parallel loss terms with transport terms to describe the parallel flow of particles and energy and ignore or keep a model like that of Eq. (1) for the perpendicular transport [20-24]. One of the major uses of these models has been in the analysis of very cool diverted plasmas, where large temperature and density gradients are observed along the field lines near the divertor.

Although the zero and one-dimensional models have proved useful, the density and temperature profiles of the edge plasma are determined by the roughly equal competition of parallel and perpendicular transport making the edge problem inherently two-dimensional. Two-dimensional models have only recently been developed [25,26]. Emery et al. [25] neglected sources due to neutral gas. The main failing of Petravic et al. [26] has been to assume that the electron conductivity is so large that there is no electron temperature gradient along the field lines. The electron heat flux Q due to conduction along the field lines can be written as $Q = \kappa_e \nabla(kT_e)$, where

$$\kappa_e = 1.21 \times 10^{20}(T_e(eV))^{5/2}(cm\ sec)^{-1}\ ,\ [27]. \qquad (3)$$

The electron conduction loss to the limiter or neutralizer plate is limited by heat transport across the sheath [7,8,28], $Q \sim 6nT_e v_f$. We can establish a minimum T_e for which conduction can keep the electron temperature gradient below a given value. Setting $\kappa_e \nabla(kT_e) = 6nvT$, we obtain ($\nabla T_e \sim \Delta T/L$, where L is a characteristic length) for a D-T plasma,

$$T_e \geq \left(4.39 \times 10^{-14} \frac{nL}{\Delta T/T}\right)^{1/2} eV\ .$$

For $\Delta T/T < 0.3$, $L \sim \pi qR = 5000$ cm, and $n = 4 \times 10^{11} cm^{-3}$, we find that $T_e \geq 17$ eV. For a denser plasma with $n = 10^{13} cm^{-3}$, $T_e \geq 85$ eV. This is less than the 800 eV predicted from the simple INTOR considerations, but higher than observed in divertor experiments with strong neutral recycling [29,30] where T_e was estimated, but not directly measured, to be below 15 eV. Our model whi.. has infinite electron conduction is thus valid for reducing T_e to ~ 20-30 eV, but begins to fail below that.

The above described models all approximate the plasma as a fluid. For the high temperature and low densities mentioned in the introduction (800 eV, $4 \times 10^{11} cm^{-3}$), the collision mean free paths are comparable to the system size, and a kinetic description may be more appropriate than a fluid description. A number of kinetic models have been constructed [31-36], including one using particle simulation techniques [34] and another solving the Boltzmann equation in one space and one velocity dimension [35]. These models may be useful in exploring the range of validity for the fluid models as well as providing better treatments of thin hot plasmas. Boozer and Auerbach [37,38] have also constructed two-dimensional fluid analytic models for diverted plasmas.

Another important ingredient for edge models is neutral atom transport. The zero-dimensional models [10,11] include many processes, such as those due to molecules and molecular ions. The usual neutral particle models [39-42] employed in one-dimensional tokamak transport codes are used for edge models based on modifications of the one-dimensional tokamak codes [13,14]. These models normally include only atomic hydrogen and calculate the neutral transport and source terms in a cylindrical geometry, although Howe [43] has recently included molecules in a one-dimensional code [44].

A variety of two-dimensional and three-dimensional neutral transport models have been developed [45-50] to compute neutral source terms in the edge. Most of these models include the transport of helium and molecular hydrogen as well as atomic hydrogen.

One important ingredient of the neutral particle transport calculations is a model for the reflection of ions and neutrals from the walls.

Measurements of reflection coefficients have been made primarily with high energy (1 keV - 10 keV ions) on smooth surfaces [51]. Calculations using the computer codes MARLOWE [52] and TRIM [53] have been used to extend the energy range down to 20 eV or so. The general features of the reflection data are that at high energies about 0.1 to 0.3 of the particles are reflected with energies of about 0.3 - 0.5 of the incident energy. The remainder of the ions or neutrals slow down and are trapped in the solid wall (Fig. 5). For normally incident particles the reflected particles are emitted with probability distributions proportional to the cosine of the angle that the outgoing particle makes with the normal to the surface. Particles that strike a smooth surface at glancing angles are more likely to undergo "specular" reflection, that is the angle of reflection is close to the angle of incidence. In this case, the probability for reflection is close to one, and the reflected particle loses little energy to the wall. Neutral particles incident at any angle on a rough surface have reflection properties like those of normally incident particles ("diffuse" reflection). The reflection properties of the neutrals have a strong effect on neutral transport through pumping ducts and divertor channels. Specular reflection will lead to a much more rapid transport of glancing neutrals down a pipe than diffuse reflection. However, real surfaces are likely to be quite complicated. They will usually be coated with impurities and probably be rough down to submicron distances.

Another ingredient is the transport of the neutrals that were not reflected after a few bounces with the solid wall, but were stopped in the bulk wall. After the wall is saturated, these neutrals will diffuse to the surface and eventually be desorbed. A time dependent model of these effects for plasma recycling has been constructed by Howe [44]. In steady state, of course, all of the neutrals that are buried in the wall will be emitted back into the plasma. Key questions are whether the absorbed neutrals are emitted or desorbed as molecules or atomic neutrals, and at what energies they are emitted.

The boundary conditions for both the neutral particle models and plasma transport calculations are determined by the electrostatic sheath that forms where the plasma flows into the limiter or neutralizer plate. The sheath potential builds up to a value sufficient to retard the electron flux so that it equals the ion flux [7,8]. The size of the potential (in the absence of secondary electron emission) is $\sim 3\ T_e$, the particle flux Γ is nv where $v = [(T_e + T_i)/n]^{1/2}$ is the sound speed and n is the average ion mass, and the electron heat flux is $2\gamma T_e\Gamma$ where $\gamma \sim 2.9$ when no secondary electron emission occurs.

With a model for plasma flow, neutral transport, neutral reflection, and boundary conditions for the sheath, one can calculate the density and temperature profiles in the edge and divertor channel, and the pumping speed of a divertor or limiter system. To assess the impurity control aspects of a divertor or pump limiter, a model for the production and transport of impurities is necessary. The most commonly accepted impurity production mechanism (at least for eroding wall materials) is physical sputtering of a surface by the bombardment of ion or neutrals.

There have been a large number of measurements of sputtering data [54]. This data has been collected into a convenient form for use in computational models [55,56]. Reference [56] is especially useful in that it contains a model for the angular dependence of the sputtering yield, as well as a prescription for calculating self-sputtering.

Calculation of the transport of impurities also requires knowing the low temperature (5–20 eV) ionization, recombination, and excitation rates for the impurities. We have used rates based on a general prescription for all elements [57]. This general data is being supplemented by better data as it appears [e.g., 58,59]. The JAERI group has used this data to model the oxygen radiation losses in the D-III expanded boundary divertor [60].

Calculations have also been performed [61,62] using one-dimensional transport codes to investigate ways to use impurity radiation at the plasma edge to cool the edge and reduce the sputtering rates. There has also been a calculation using a three-dimensional neutrals code to investigate the enhancement of impurity radiation at the edge due to charge-exchange recombination [63].

One new area has been the theoretical investigation of molecular effects in the transport of impurities [64]. The basic idea was that slow (~ 0.1 eV) neutral carbon would penetrate roughly one electron ionization mean free path into a discharge. Methane evolved from the wall would have roughly the same energy as a neutral carbon atom. However, it would be ionized and dissociated in the following chain of events:

$$C^o + e^- \rightarrow C^+ + 2e^-$$

and

$$CH_4 + e^- \rightarrow CH_4^+ + 2e^-$$
$$CH_4^+ + e^- \rightarrow CH_3^+ + 2e^-$$
$$CH_3^+ + e^- \rightarrow CH_2^+ + 2e^-$$
$$CH_2^+ + e^- \rightarrow CH^+ + 2e^-$$

$$CH^+ + e^- \rightarrow \begin{matrix} C^+_o + H^+_+ + 2e^- \\ C_o + H_o + e \\ C^o + H^o \end{matrix}$$

The time for this succession of ionizations and dissociations is comparable to the thermal equilibration time with the 5-30 eV ions in the edge plasma. This can result in "boosting" the carbon energy from ~ 0.1 eV to several eV, thus increasing the ionization mean free path by as much as a factor of 10. For some edge conditions this can lead to an enhancement of the carbon penetration for methane produced carbon compared to atomic carbon while also leading to a return of some carbon to the wall.

In summary, the ingredients are becoming available for reasonable quantitative models for the edge plasma. For the rest of the paper we will describe some of the models we use, and how we use those models in an attempt to interpret present experiments and extrapolate to larger experiments such as INTOR. A great deal of work on the INTOR divertor design has been done by the various design teams from the USSR, Japan, and Europe as well as the United States, but we will concentrate on our work at Princeton.

III. TWO-DIMENSIONAL NEUTRAL TRANSPORT CALCULATIONS

The transport of neutrals in a typical divertor geometry is inherently at least a two-dimensional problem. As we have seen in the previous section, a neutral transport model not only provides information about the wall erosion and pumping rates, but provides the source terms for a plasma computation. The ionization of neutrals serves as a source of plasma density and a cooling (or heating) term for the ions and electrons, and also dilutes the momentum of the plasma. Charge exchange does not affect the density, but does exchange energy and momentum between the divertor walls and the plasma, and between various parts of the plasma. We will see in Section IV that the inclusion of reactions with neutrals, particularly ionization, can produce dramatic changes in the plasma parameters in a divertor.

Given the two-dimensional nature of the problem, plus the need for a kinetic treatment of the particles, most researchers have chosen to use Monte Carlo techniques. The pioneering work in this field was performed by a group at JAERI [34,47], who were the first to study the problem of helium and hydrogen transport in a diverted plasma. A year later a similar code was written at PPPL [46,65], and shortly thereafter other calculations were in progress [48,49].

The two significant physics ingredients to our neutral particle code (in addition to the numerical techniques) are the atomic physics of the neutral-plasma collisions, and the wall reflection model for the neutrals.

The collision processes included in our code are listed in Table I. The code follows H, D, T, their associated molecules, H_2, D_2, T_2, HD, HT, and DT, and He. Reactions such as

$$e^- + H_2^o \rightarrow H^+ + H^+ + 3e^- ,$$
$$e^- + H_2^+ \rightarrow H^+ + H^+ + 2e^- ,$$

have appreciably smaller cross sections than competing reactions, and so are not included.

The cross sections for the reactions in Table I are computed from the polynomial formulae in Freeman and Jones [66] and Jones [67], which are used to compute tables of $\langle\sigma v\rangle$ as a function of neutral energy E_o and plasma ion temperature T_i, using Gauss-Hermite quadrature.

A measure of the relative importance of each reaction can be obtained from the reaction rates $n\langle\sigma v\rangle$ where n is a typical density chosen for the plasma ions (D^+, T^+, or He^{++}) or electrons (Figs. 6a, 6b, 6c). The dominant reaction for neutral hydrogen at all energies is charge exchange (Fig 6b).

Ionization for neutral hydrogen is almost comparable to charge exchange at T ~ 40-60 eV, but it is much less important at lower temperatures. This contrasts with the situation for neutral helium where ionization dominates helium-helium charge exchange for T > 4 eV. Helium-hydrogen charge exchange is important only at high temperatures (> 2 keV).

The relative neutral/ion yield rates from H_2^o dissociations by electrons are plotted in Fig. 7 as a function of electron temperature T_e. For $T_e < 10$ eV, the dominant reaction is $e + H_2^o \rightarrow 2H^o + e$ so that almost all dissociating hydrogen is atomic. Above ~ 10 eV, electron ionization followed by dissociation into $H^o + H^+ + e$ becomes important, and, for $T_e > 100$ eV, half the hydrogen produced by dissociation is atomic and the other half is ionized. Also, since the velocity of the molecules is low (~ 10^5cm/sec) having been desorbed off a wall, the mean free path of the molecules is shorter than the mean free path of energetic hydrogen neutrals (~ 3 eV, v ~ 10^6cm/sec). This results in about one-half of the hydrogen atoms that leave the wall as molecules being ionized very close to the wall.

Three wall reflection models are used. What is required for each incident particle with a given incident energy and angle to the normal is an algorithm for picking the outgoing energy and angles of emission. The first model uses a data base compiled from many MARLOWE [52] computations. The second model is taken from Seki [47] for an iron surface. The reflected velocities vary from specular (angle of incidence equals angle of reflection) for glancing collisions to a cosine distribution for normally incident particles. The third model reflects all particles with a cosine distribution and is probably the best suited for rough walls. The reflected energy is degraded in the last two models as is done in Seki [47].

Hydrogen and helium not reflected is assumed to desorb eventually (in steady state) as molecules or atoms, mono-energetically at the wall temperature, and with a cosine distribution in polar angle. Molecules striking the wall do so at low velocity and are assumed to desorb immediately with the a cosine distribution.

The ordering of reaction rates for hydrogen and helium is important for the relative transport of neutral hydrogen versus neutral helium in a plasma. It has been argued [47] that the plasma acts as a helium filter. Since neutral hydrogen atoms can charge exchange with the hot ions in the plasma, some of the energy lost by collisions with the wall can be recovered by the neutral hydrogen atoms, and thus keep the mean free path for ionization large. Helium atoms, however, would be "re-energized" by charge exchange to a much lesser degree than hydrogen. This is because the charge-exchange cross sections for helium with helium are smaller than for hydrogen with hydrogen, and the percentage of helium ions in the plasma is small (~ 5% of n_e) compared with hydrogen (~ 90% of n_e) (Fig. 6c). Thus, the helium atoms would be expected to slow down by wall collisions and might be ionized more rapidly than the hydrogen atoms.

The situation is complicated, however, by the fact that the hydrogen mean free path for charge exchange is about one-half of the mean free path for ionization. Thus there will be about two charge-exchange collisions for each ionizing collision. If we assume that neutral hydrogen atoms resulting from charge-exchange collisions are isotropically distributed, the directed motion of neutrals down the divertor duct will be lost. Charge exchange for hydrogen thus helps the transport of hydrogen neutrals down the divertor by restoring the energy lost by wall collisions, but it also retards the transport by randomizing the velocities of the neutral atoms. Further complicating the picture is the lower ionization rate of helium compared to hydrogen and the production of cold hydrogen molecules at the wall (as just described). We have found that for INTOR the net result of all these competing effects is that hydrogen and helium neutrals have similar transport rates at moderate plasma densities (~ 10^{12} - 10^{13} cm^{-3}). Seki et al. [47] have found (Fig. 8) the backflow $B = [\Gamma_{plasma}/(\Gamma_{plasma} + \Gamma_{pump})]$ in their calculation varied from 0.46 to 0.7 for DT, and from 0.23 to 0.7 for He as the density varied from 4×10^{11} cm^{-3} to 8×10^{12} cm^{-3}. Thus, the helium enrichment they calculate varies from 2 to 1. In particular, their result for a density of 3×10^{12} cm^{-3} has an enrichment of $B_H/B_{He} = 1.13$. Our case at that density yields backflows of 0.34 for D, 0.31 for T, and 0.44 for He (Table II). This is a helium de-enrichment of $B_H/B_{He} = 0.75$ [46,65]. However, considering the uncertainties in the wall reflection models, the different atomic physics, and differences in the codes, this discrepancy probably is not significant.

What is clear is that significant helium enrichment (factors of 5 or more) probably does not exist. This conclusion is consistent with recent measurements on D-III [68].

Calculated neutral conductances for a variety of divertor conditions is given in Table II [46]. The density in the first three cases was 8.8×10^{12} cm^{-3} at the center, falling to 1.1×10^{12} cm^{-3} at the channel walls. The central electron temperature was 250 eV with the same Gaussian profile as the density. Two things are worth noting. The first is that helium de-enrichment was found for all cases. The second is that the gas throughputs are higher than might be expected naively.

The conductances (pumping speeds) of the pumping ducts were computed with the code and compared with the classical Clausing values [69] using a neutral temperature of 300°k. The actual pumping speed was much higher than the Clausing value. The results from the code indicated that the neutrals formed near the plate are energetic, and flow down the duct, cooling by collisions with the pump duct walls. Thus, the effective temperature of the neutrals is high. The actual throughput is somewhere between equal fluxes ($\sim \sqrt{E}$) and equal pressures ($\sim E$). It is this "enhanced" pumping that is probably responsible for part of the high neutral pressures observed at ends of pumping ducts which are placed near surfaces where the plasma is recycling [70]. Most of the neutrals that flow toward the main plasma are ionized in the divertor plasma.

The other types of information the neutral code can provide are heat loads, total sputtering rates, and the energy, momentum and particle source rates useful to a solution of the plasma flow equations.

IV. TWO-DIMENSIONAL PLASMA FLOW MODELS

The large ionization rates in the plasma will affect the diverted plasma. To examine the effects of the neutral collisions on the plasma, we have constructed a two-dimensional model for the flow of a one ion species plasma in a poloidal divertor [26]. In this model, we solve steady state equations for the transport of particles, momentum, and energy. In Cartesian coordinates (Fig. 9), these equations we use have the form

$$\frac{\partial(nv_\xi)}{\partial\xi} = S_n(\xi,y) + \frac{\partial}{\partial y}\left(D\,\frac{\partial n}{\partial y}\right) , \tag{3}$$

$$\frac{\partial}{\partial\xi}\left[n\left(mv_\xi^2 + T_i + T_e\right)\right] = S_p(\xi,y) + \frac{\partial}{\partial y}\left(mv_\xi D\,\frac{\partial n}{\partial y}\right) , \tag{4}$$

$$\frac{\partial}{\partial\xi}\left[nv_\xi\left(\frac{5}{2}\,T_i + \frac{1}{2}\,mv_\xi^2\right)\right] = -v_\xi T_e\,\frac{\partial n}{\partial\xi} + S_{E_i}(\xi,y) + \frac{\partial}{\partial y}\left(\left[\frac{5}{2}\,T_i + \frac{1}{2}\,mv_\xi^2\right]D\,\frac{\partial n}{\partial y}\right), \tag{5}$$

$$\frac{\partial Q_e}{\partial\xi} = v_\xi T_e\,\frac{\partial n}{\partial\xi} + S_{E_e}(\xi,y) + \frac{\partial}{\partial y}\left[\left(\frac{3}{2}\,T_e\right)D\,\frac{\partial n}{\partial y}\right] . \tag{6}$$

Electron inertia has been neglected and the electric field has been eliminated through charge neutrality and electron pressure balance. The S's are the density, momentum, ion energy and electron energy source terms, respectively, due to charge exchange, ionization, and radiation of the neutral gas. ξ is the coordinate along the field line, y is the coordinate perpendicular to the flux surface, and D is the perpendicular diffusion coefficient.

The boundary conditions at the sheath are that the heat flux Q and particle flux Γ are given by $Q_e^{sh} = 2\gamma T_e (nv_s)^{sh} (\gamma \sim 2.9)$, $\Gamma = nv_s$, and v_s^{sh}, the plasma flow velocity computed at the sheath boundary, is obtained from $(1/2)\ mv_s^2 = (5/6)\ T_i + (1/2)\ T_e$. The input fluxes of particles and energy are specified at the divertor throat. One key point is that the plasma flows at the local sound speed at the sheath boundary. T_e is assumed constant along the field lines, an assumption of limited validity as we have seen. The neutral source terms are obtained self-consistently from the code [46] described in the previous section.

We have used the code to explore possible operating parameters for poloidal divertors. We have found that the divertor operating regime depends on the degree of neutral recycling that takes place in the divertor chamber. We studied this effect for a PDX-like geometry by varying the pumping speed near the neutralizer plate of the divertor chamber [26] (Fig. 9). This was accomplished by varying the pump opening, δ, (Fig 9) from 2 to 6 cm. For small δ, few neutrals could escape down the pump, and most would be ionized in the diverted plasma or escape back to the main plasma. The heat flux corresponded to 8 MW of neutral beam injection (2 MW/plate), and the particle flux corresponded to a particle confinement time of 30 milliseconds. The cross-field diffusion was set to ~ 5% of Bohm diffusion and was small compared to the parallel flow. The results for $\delta = 4$ cm are illustrated in Fig. 10.

The source of neutrals due to ionization is localized near the plate. From the continuity equation (3), it can be seen that since $S > 0$, the particle flux $\Gamma = nv$ increases along the field line from the input value to a larger value at the plate. For $\delta = 4$ cm, this increase is roughly a factor of 4. The calculations indicate that Q_i and Q_e are not significantly decreased by charge exchange, ionization or radiation. Thus, at the sheath boundary, $Q_x \sim 8Tnv_x$ (projected into the poloidal cross section with $Q_x/Q_\xi \sim 0.1$). Since $\Gamma_x = nv_x$, $Q_x/\Gamma_x = 8T$ and raising Γ_x by a factor of 4 lowers $\acute{T}$ at the plate by a factor of 4 compared to the case with no neutral recycling. Each particle gets four times as many chances to carry the heat flux to the plate as it would if there were no recycling. Since $Q_x \sim Tn\sqrt{T/M}$, $nT^{3/2} =$ constant. Thus a decrease in T at the plate results in an increase in n at the plate. This is illustrated by computing the divertor parameters as a function of pump opening (Fig. 11). As the pump opening is decreased from 6 cm to 2 cm, the recycling particle flux at the plate increases. The temperatures decrease, the densities increase, and the neutral pressure increases. Quite high pressures and densities can be obtained (100 microns, 10^{14}cm^{-3}) which are roughly consistent with measurements on D-III [22,29,30,68] and Alcator [70]. Attempts to reduce the pump opening below 2 cm results in a lack of convergence for our numerical method.

These results allow us to divide divertor operation into roughly three regimes characterized by the amount of neutral recycling in the divertor [Table III]. The first regime is characterized by very little recycling. The temperatures are high and the densities are low, as would be predicted from simple sheath theory. The neutrals can easily escape down the pump or back to the main plasma without being ionized. The neutral pressure is low.

The second regime is characterized by a medium level of recycling. The ratio of the plate flux to the throat flux is between 1 and 10. The density is in the $10^{13}cm^{-3}$ range, and for typical heat fluxes and particle fluxes (beam heated), the temperature is about 50-100 eV. The neutral pressure at the plate is around 10^{-3} torr. The neutral mean free path is shorter than the length of the divertor channel, but longer than the width of the divertor, so that neutrals can escape down the pump but not back to the main plasma. Radiation from hydrogen and charge exchange does not transfer much of the heat flux to the divertor walls before the plasma reaches the neutralizer plate. The sputtering yields are high in both regimes since the ion energies are above the sputtering thresholds for realistic materials. In fact, due to the higher particle flux in the intermediate recycling regime, the total erosion rates may be higher than those for the low recycling regime. Experiments with outside limiters and open divertor geometries like PDX are probably between the first and second regime, since even with a limiter there is some local recycling.

The third regime is characterized by large recycling rates. Each ion typically recycles ten times or more before being pumped or reaching the main plasma. The neutral mean free paths are short compared to both the length and width of the divertor. The electron temperature is below 30-40 eV and the density is high ($\sim 10^{14}cm^{-3}$). The neutral pressure is high ($\lesssim 10^{-2}$ torr). At these densities radiation and charge exchange begin to be important. The temperature may also be low enough that significant electron temperature gradients along a field line can be supported. Because of the low temperature, which leads to a low sputtering rate, and a high neutral pressure, which leads to large gas throughputs for modest sized pumping systems, this regime is the best one for a large tokamak. Our code has only been able to partially enter this regime ($T \sim 20$ eV, $n \sim 10^{14}$ cm^{-3}) due to our neglect of electron temperature gradients, use of approximate radiation treatments, and the fixed input flux boundary conditions. This high recycling regime, however, has been observed on D-III [22,29,30,68]. Although the expanded boundary type of divertor on D-III [71] is open at the sides, the width is large on D-III (10-30 cm) which is large enough to ionize most of the neutrals which hit the wall, thus achieving a high recycling rate. Recent observations on D-III support the role of recycling and hydrogen radiation in the operation of their high density divertor [72].

One key feature of the calculations with appreciable recycling is that the plasma flow velocity is a maximum at the divertor plate. Since the flow (nv) rises toward the plate, and v at the plate is fixed at the sound speed, part of the flux rise comes from an increase in v along the field line. Thus, the flow velocity at the divertor throat is less than the sound speed at the plate, and much less (10^{-2} - 10^{-1}) than the sound speed at the throat (Fig. 12).

The flow speed of C II was measured in the divertor on PDX. As the density in the divertor increased (as indicated by H_α emission), the C II flow speed dropped from sonic ($\sim 2 \times 10^6$ cm/sec) to a much smaller value ($\lesssim 10^5$ cm/sec) [74]. In PDX [74], ASDEX [75,76], and D-III [30], the line density in the divertor is observed to rise as n_p^α where n_p is the main plasma line density and $\alpha \gtrsim 2$. These results qualitatively indicate the importance of recycling in the divertor.

V. FUTURE DIRECTIONS

The general quality of models for divertors will continue to improve during the next few years, especially as divertor and pump limiter experiments are analyzed. The fluid model presented in Section IV has a number of shortcomings. The key physics ingredients omitted were an electron temperature gradient along a field line, a general geometry, a general set of boundary conditions that included the main plasma in a self-consistent fashion, a realistic treatment of the hydrogen line radiation and an impurity transport treatment. Some of these shortcomings are being corrected [77] in our model.

It is also important to have derived a consistent and complete set of equations for the plasma flow at the plasma edge. Early attempts to do this made simplifying assumptions which limited their applicability for practical problems [37,38,26]. A more complete analysis has been conducted by Singer and Langer [78] for the high collisionality regime, which is optimal for a high recycling divertor in a tokamak reactor, where the Mach number is much less than one for almost all of the plasma. They find that in addition to the terms treated in [77], loss of particles and energy by diamagnetic flows must be included, as well as viscosity and Coriolis forces. With these ingredients, we hope that we can explore quantitatively the parameters for the kinds of cool dense plasmas observed on D-III. Recently, there have been observations of a cool dense plasma layer on the inside limiters of D-III [72] and Alcator C [79]. These may be manifestations of the effects of high recycling found to be important for divertors.

The next big step after this will be the inclusion of impurities, impurity production, transport and radiation. Already there have been calculations of impurity transport near limiters [80]. Coupled with impurity injection experiments these models might allow one to begin to construct a quantitative model for impurity behavior in the plasma edge.

Such progress is promising not only because the plasma-wall interaction is the source of most impurities, but because a real understanding of impurity behavior in the edge may allow the use of impurity radiation to help keep the edge cool. Edge cooling by impurity radiation has been proposed by many, but no truly convincing scenario yet exists.

Another exciting development has been the work examining the boundary conditions for the electrostatic sheath that forms when the field lines make shallow angles with the neutralizer plate [81-83]. In fact, the level of general progress in edge models has been such that for the first time constructing a comprehensive model begins to make sense.

In some ways, the experimental and theoretical progress in divertors, limiters, and pump limiters has been one of the most optimistic developments for the tokamak program in the last three years. When the INTOR effort began, the pumping and impurity control problems seemed insurmountable. It now appears that there are experimental and theoretical grounds to believe that cool, dense diverted and maybe even limited plasmas may be able to solve these problems.

ACKNOWLEDGMENTS

The authors are grateful to Glen Bateman, Alan Boozer, William Langer, Paul Rutherford, John Schmidt, Cliff Singer, and Jon Weisheit for encouragement and assistance, and to Mrs. E. Carey for assistance in preparing the manuscript.

This work was supported by the U.S. Department of Energy Contract No. DE-AC02-76-CHO-3073.

REFERENCES

[1] L. Spitzer, Report No. NYO-993, USAEC, Washington, DC (1951); see also Phys. Fluids 1, 253 (1958).

[2] D. Meade et al., Fifth International Conference on Plasma Physics and Controlled Nuclear Fusion Research, Tokyo (1974).

[3] M. Keilhalker, Magnetic Divertors, IPP-III/33, November 1976, Max-Planck-Institut Für Plamsaphysik, Garching.

[4] A Fusion Power Plant, R. G. Mills, Editor, MATT-1050, Princeton University, Plasma Physics Laboratory, August 1974.

[5] A. T. Mense, Ph.D. Thesis, University of Wisconsin, UWFDM-219 (1977).

[6] INTOR Group, Nuclear Fusion 22, 135 (1982).

[7] G. D. Hobbs and J. A. Wesson, Plasma Physics 9, 85 (1982).

[8] L. Tonks and I. Langmuir, Phys. Rev. 34, 876 (1929).

[9] R. Hawryluk and J. Schmidt, Nucl. Fus. 16, 775 (1976).

[10] F. Marcus, private communication.

[11] M. Gordinier and R. Conn, J. of Nuc. Mat. 93 and 94, 420 (1980).

[12] P. Raimbrult and J. P. Girard, Physics Scripta 23, 107 (1981).

[13] A. Mense and G. A. Emmert, Nucl. Fus. 19, 361 (1979).

[14] J. Ogden et al., IEEE Transactions on Plasma Science, PS-9, 274 (1981).

[15] G. Becker and C. Singer, "Simulation of Plasma Transport in the Scrape-off Region of Asdex," IPP-III/75, November 1981, Max Planck Institute Für Plasmaphysik, Garching.

[16] J. Hogan, Methods in Computational Physics, Vol. 16, Controlled Fusion, (Academic Press 1976) p. 131.

[17] D. Düchs, D. Post, and P. Rutherford, Nucl. Fus. 17, 565 (1977).

[18] A. Nedospasov and M. Tokar, Nucl. Fus. 21, 465 (1981).

[19] D. Anderson, M. Lisak, and H. Wilhemsson, Nucl. Fus. 19, 1523 (1979).

[20] M. Shimada et al., JAERI M-9470, Japan Atomic Energy Research Institute, April 1981.

[21] J. Morgan and P. Harbour, "Modelling of Divertor Flow For a Reactor Regime," Fusion Technology, Vol. 2, 1187 (Pergammon Press 1980), Oxford, Great Britain.

[22] M. Ali Mahdavi, J. De Boo, C. Hsieh, N. Ohyabu, R. Slanbaugh, and J. Wesley, Phys. Rev. Lett. 47, 1602 (1981).

[23] K. Lackner and W. Schneider, International Conference on Plasma Physics, Goteborg, Sweden, June 1982 (to be published).

[24] G. Proudfoot and P. Harbour, paper F4, this meeting.

[25] M. Emery, J. Gardner, M. Fritts, J. Boris, and N. Winsor, "A General Two-Dimensional Tokamak Model," NRL Report 3744, Naval Research Laboratory, Washington, DC, March 1978.

[26] M. Petravic, D. Post, D. Heifetz, and J. Schmidt, Phys. Rev. Lett. 48, 326 (1982).

[27] D. Book, NRL Plasma Formulary, Naval Research Laboratory, 1980.

[28] G. A. Emmert, R. M. Weiland, A. T. Mense, and J. N. Davidson, Physics of Fluids 23, 803 (1980).

[29] N. Nagami et al., IAEA-CN-38/0-2, Eighth International Conference on Plasma Physics and Controlled Fusion Research, Brussels, Belgium, July 1-10, 1980.

[30] M. Ali Mahdavi et al., "Properties of Diverted Plasmas with Magnetically Expanded Flux Surfaces," GA-A15963, General Atomic Company, July 1980.

[31] U. Daybelge, Nucl. Fus. 21, 1589 (1981).

[32] F. L. Hinton and R. D. Hazeltine, Phys. Fluids 17, 2236 (1974).

[33] H. A. Claussen and H. Repp, Nucl. Fus. 21, 5896 (1981).

[34] T. Takizuka et al., IAEA-CN-38/X-2-1, Eighth International Conference on

Plasma Physics and Controlled Nuclear Fusion Research, Brussels, Belgium, July 1-10, 1980.

[35] P. Gierszewski, P. McKentz, J. McCallen, and R. Morse, "Structure of Wall Plasmas Near Divertor Neutralizer Plates or Limiters," (submitted to Phys. Rev. Lett, October 1980).

[36] A. Bailey and G. Emmert, paper F22, this meeting.

[37] A. H. Boozer, Phys. Fluids 19, 1210 (1976).

[38] S. Auerbach and A. H. Boozer, Phys. Fluids 23, 1297 (1980).

[39] M. Hughes and D. P[illegible], J. Comp. Phys. 28, 43 (1978).

[40] G. Emmert and K. Audenaerde, J. Comp. Phys. 34, 268 (1980).

[41] K. Burrell, J. Comp. Phys. 27, 88 (1978).

[42] S. Tamor, J. Comp. Phys. 40, 104 (1981).

[43] H. Howe, paper F33, this meeting.

[44] H. Howe, J. of Nuc. Mat. 93, and 94, 17 (1980).

[45] D. Heifetz and D. Post, "Seurat, A Two-Dimensional Neutral Gas Transport Code (submitted to Comp. Phys. Comm.)

[46] D. Heifetz, D. Post, M. Petravic, J. Weisheit and G. Bateman, "A Monte Carlo Model of Neutral Particle Transport in Diverted Plasmas," PPPL-1843, November 1981 (to be published in J. Comp. Phys.).

[47] Y. Seki et al., Nucl. Fus. 20, 1213 (1980).

[48] E. Cupini, A. DeMattis, and R. Simonini, "Monte Carlo Neutral Transport in Plasma, A Preliminary Study," January 1982 (unpublished).

[49] A. Nicolai and D. Reiter, paper F30, this meeting

[50] J. Hogan, paper F25, this meeting.

[51] W. Eckstein and H. Verbeek, "Data on Light Ion Reflection," IPP9/32, Max Planck Institut Für Plasmaphysik, Garching, August 1979.

[52] M. T. Robinson et al., Phys. Rev. B9, 5008 (1974).

[53] J. P. Biersack and L. G. Haggmark, to be published.

[54] J. Bohdansky, J. of Nucl. Mat. 93 and 94, 45 (1980).

[55] J. Bohdansky, J. Roth and H. L. Bay, J. Appl. Phys. 51, 2861 (1980).

[56] D. L. Smith, J. N. Brooks, and D. E. Post, "A Physical Sputtering Code for Fusion Applications," Proceedings of the Ninth Symposium of Engineering Problems of Fusion Research, Chicago, Illinois, October 26-29, 1981.

[57] D. Post, R. Jensen, C. Tarter, W. Grasberger, and W. Lokke, At. Data and Nucl. Data Tables 20, 397 (1977).

[58] K. Bell, H. Gilbody, J. Hughes, A. Kingston, and F. Smith, "Recommended Data on the Electron Ionization of Light Atoms and Ions," to appear in J. of Phys. and Chem. Ref. Data.

[59] M. S. Pindzola and D. H. Crandall, "A Compilation of Theoretical Electron-Impact Excitation Cross Sections for Fe Atomic Ions," ORNL/TM-957, November 1981, Oak Ridge National Laboratory.

[60] M. Shimada et al, JAERI-M9862, December 1981, Japanese Atomic Energy Research Institute.

[61] A. Gibson and M. Watkins, Proceedings of the Eighth European Conference on Controlled Fusion and Plasma Physics, Prague, 1, 31 (1977).

[62] J. Neuhauser, "Characteristics of a Radiating Layer Near the Boundary of a Contaminated Plasma," IPP-1/182, August, 1980.

[63] J. Hogan, Physics of Electronic and Atomic Collisions, S. Datz, Editor, North Holland Publishing Co., 1982.

[64] W. Langer, "Transport of Molecular Impurities at the Edge of Tokamaks," PPPL-1856, November 1981, to be published in Nuclear Fusion.

[65] J. D. Callen et al., IAEA-CN-38-Y-3, Eighth International Conference on Plasma Physics and Controlled Nuclear Fusion Research, Brussels,

Belgium, July 1-10, 1980.

[66] R. L. Freeman and E. M. Jones, CLM-R137, Culham Laboratory, Abingdon, Berkshire (1974).

[67] E. M. Jones, CLM-R175, Culham Laboratory, Abingdon, Berkshire (1977).

[68] M. Shimada et al., Phys. Rev. Lett. 47, 796 (1981).

[69] P. Clausing, Ann. Physik 12, 961 (1932).

[70] D. Overskei, Phys. Rev. Lett. 46, 177 (1981).

[71] N. Ohyabu, Nucl. Fus. 21, 519 (1981).

[72] N. Ohyabu, D. Baker, M. Brooks, J. DeBoo, and M. Ali Mahdavi, "Density Oscillation in the Tokamak Plasma Boundary with an Expanded Divertor Channel," GA-A16484, General Atomic Company, January 1982.

[73] D. Post, M. Petravic, J. Schmidt, and D. Heifetz, J. Vac. Sci. and Tech. 20, 1242 (1982).

[74] R. Fonck et al., paper E3, this meeting.

[75] W. Englehardt et al., paper E2, this meeting.

[76] M. Keilhacker et al., paper 1R3, Proceedings of IAEA Technical Committee Meeting on Divertors and Impurity Control, Garching, Germany, July 6-10, 1981.

[77] M. Petravic, D. Post, and D. Heifetz, paper C7, this meeting.

[78] C. Singer and W. Langer, paper F18, this meeting.

[79] J. Terry et al., Bull. Am. Phys. Soc. 26, 886 (1981).

[80] J. Brooks, paper F19, this meeting.

[81] J. Brooks, "Kinetic Solution of the Sheath Region in a Fusion Reactor," ANL/FPP/TM-124, Argonne National Laboratory (1979).

[82] R. Chodura, "Plasma Wall Transition in an Oblique Magnetic Field," IPP-1/194, October 1981, Max Planck-Institut Für Plasmaphysik, Garching.

[83] C. Daybelge and B. Bein, Phys. Fluids 24, 1190 (1981).

TABLE I

(1)	H^o	$+ H^+$	$\rightarrow H^+$	$+ H^o$	
(2)	e	$+ H^o$	$\rightarrow H^+$	+ 2e	
(3)	e	$+ H_2^o$	$\rightarrow 2H^o$	+ e	
(4)	e	$+ H_2^o$	$\rightarrow H^o$	$+ H^+$	+ 2e
(5)	e	$+ H_2^o$	$\rightarrow H_2^+$	+ 2e	
(5a)	e	$+ H_2^+$	$\rightarrow 2H^o$		
(5b)	e	$+ H_2^+$	$\rightarrow H^o$	$+ H^+$	+ e
(6)	He^o	$+ He^+$	$\rightarrow He^+$	$+ He^o$	
(7)	He^o	$+ He^{++}$	$\rightarrow He^{++}$	$+ He^o$	
(8)	He^o	$+ H^+$	$\rightarrow He^+$	$+ H^o$	
(9)	e	$+ He^o$	$\rightarrow He^+$	+ 2e	

Neutral-Plasma Reactions Included in Our Model. H is hydrogen, deuterium, or tritium. We assume that if H_2^o is ionized in reaction (5), then the H_2^+ produced is dissociated instantaneously by reactions (5a) or (5b).

TABLE II

ℓ (cm)	a (cm)	Q_p/Q_t D	T	He	E	R_{vac}	$C = (Q_p/Q_t)/R_{vac}$ DT	He
80	30	2.67	3.83	0.56	5.80	0.20	16.3	2.8
50	30	0.53	0.70	0.25	2.46	0.16	3.9	1.6
50	40	0.26	0.39	0.13	2.50	0.11	3.0	1.1
100	30	1.94	2.20	1.23	1.68			

Relative pumping rates for D, T, and He in rectangular divertors [46]. Divertor throats are ℓ by a cms, and pumps are 40 cm by a cm. Q_p and Q_t are the currents leaving the pump and throat, respectively. E is the ratio Q_p/Q_t for DT over Q_p/Q_t for He. R_{vac} is the ratio of pump to throat conductances computed for a vacuum using Clausing's formula [69] and C is Q_p/Q_t over R_{vac}.

TABLE III

Approximate Divertor Operating Regimes for a Divertor of Length b and Width a (INTOR Heat Fluxes and Particle Fluxes)

Neutral Recycling	Low	Medium	High
$\lambda_o = n_e \langle \sigma v \rangle_{ionize}$ Neutral Mean Free Path	$\lambda_o > a, b$	$b > \lambda_o > a$	$b, a > \lambda_o$
$R = \Gamma_{plate}/\Gamma_{throat}$	$R \sim 1$	$1 \lesssim R \lesssim 10$	$R \gtrsim 10$
T_e	200-1000 eV	30-200 eV	< 30 eV
Edge Plasma Density	10^{11}-10^{12}cm^{-3}	10^{13}cm^{-3}	10^{14}cm^{-3}
Importance of Hydrogen Radiation	negligible	~ 10%	10-90% (Est.)
Neutral Pressure	10^{-6}-10^{-4} torr	10^{-4}-10^{-2} torr	> 10^{-2} torr
Electron Temperature Gradient	small	~ 10%	large

FIGURE CAPTIONS

Fig. 1. Schematic of a poloidal divertor (taken from Dale Meade, private communication).

Fig. 2. Schematic of plasma flow in a divertor (taken from [46]).

Fig. 3. Types of physics involved in a divertor for a high beta plasma.

Fig. 4. Parameters in the scrapeoff plasma for INTOR calculated with model in Ref. 14. The separatrix is at r = 152 cm.

Fig. 5. Schematic illustration of neutral atoms and ions colliding with a surface.

Fig. 6a. $n\langle\sigma v\rangle$ For

(1) $H^o + H^+ \rightarrow H^+ + H^o$, $n = n_{H^+} = 1 \times 10^{13}\ cm^{-3}$

(2) $e^- + H^o \rightarrow H^+ + 2e^-$, $n = n_e = 1.1 \times 10^{13}\ cm^{-3}$

(3) $e^- + He^o \rightarrow He^+ + 2e^-$, $n = n_e = 1.1 \times 10^{13}\ cm^{-3}$

(4) $He^o + He^{++} \rightarrow He^{++} + He^o$, $n = n_{He^{++}} = 0.05 \times 10^{13}\ cm^{-3}$

(5) $He^o + H^+ \rightarrow He^+ + H^o$, $n = n_{H^+} = 1 \times 10^{13}\ cm^{-3}$

where H = D/T, $E_{H^o} = 3 \times T_e$, $E_{He^o} = 6 \times T_e$, and $T_i = T_e$.

Fig. 6b. Hydrogen and helium charge exchanging probabilities, $T_i \approx T_e$ (compared to ionization).

Fig. 6c. $n_e\langle\sigma v\rangle$ for

(1) $e^- + H_2^o \rightarrow H_2^+ + 2e^-$

(2) $e^- + H_2^o \rightarrow 2H^o + e^-$

(3) $e^- + H_2^o \rightarrow H^o + H^+ + 2e^-$

(4) $e^- + H_2^+ \rightarrow 2H^o$

(5) $e^- + H_2^+ \rightarrow H^o + H^+ + e^-$

assuming $n_e = 1.1 \times 10^{13}\ cm^{-3}$.

Fig. 7. *H^o and H^+ yield fractions from H_2^o dissociation.*

Fig. 8. Backflow fraction as a function of divertor density [47].

Fig. 9. Model divertor chamber. The length of the chamber is 40 cm and the width is 6 cm. The plasma is 4 cm wide. (Taken from [26]).

Fig. 10. Calculated plasma parameters along the separatrix in the modified PDX divertor for a pump opening of 4 cm. (Taken from [26]).

Fig. 11. The neutral pressure P_0, the plasma density at the throat and at the plate n_e, the ion temperature at the plate T_i, the electron temperature T_e, and the total particle flux Γ at the plate, Γ at the plate as a function of the pump opening for the divertor chamber in Fig. 9 and for the PDX-like conditions described in the text. (Taken from [26]).

Fig. 12. The fluid velocity along the field line projected into the poloidal cross section for an INTOR divertor design. (Taken from [73]).

POLOIDAL DIVERTOR MAGNETICS

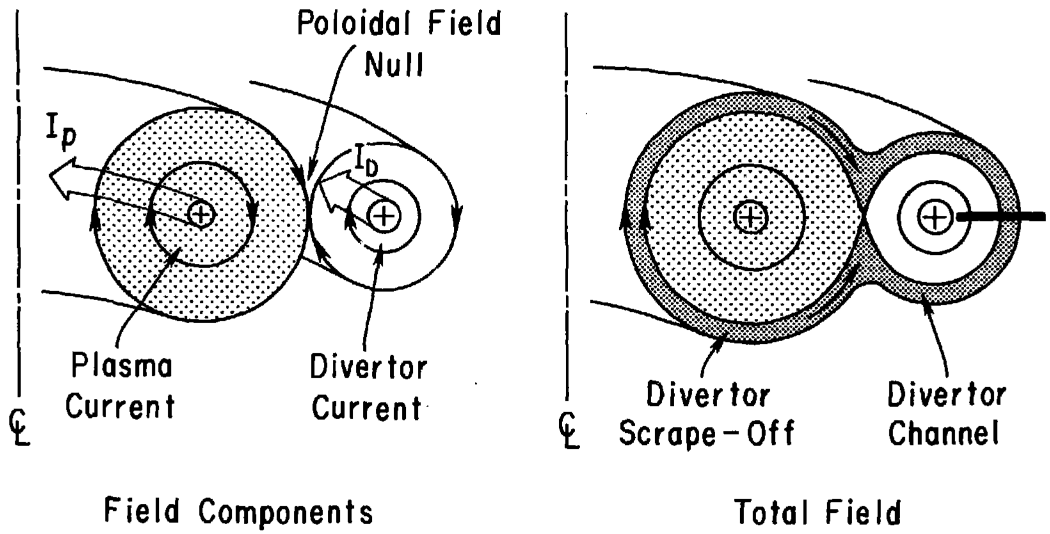

FIG. 1

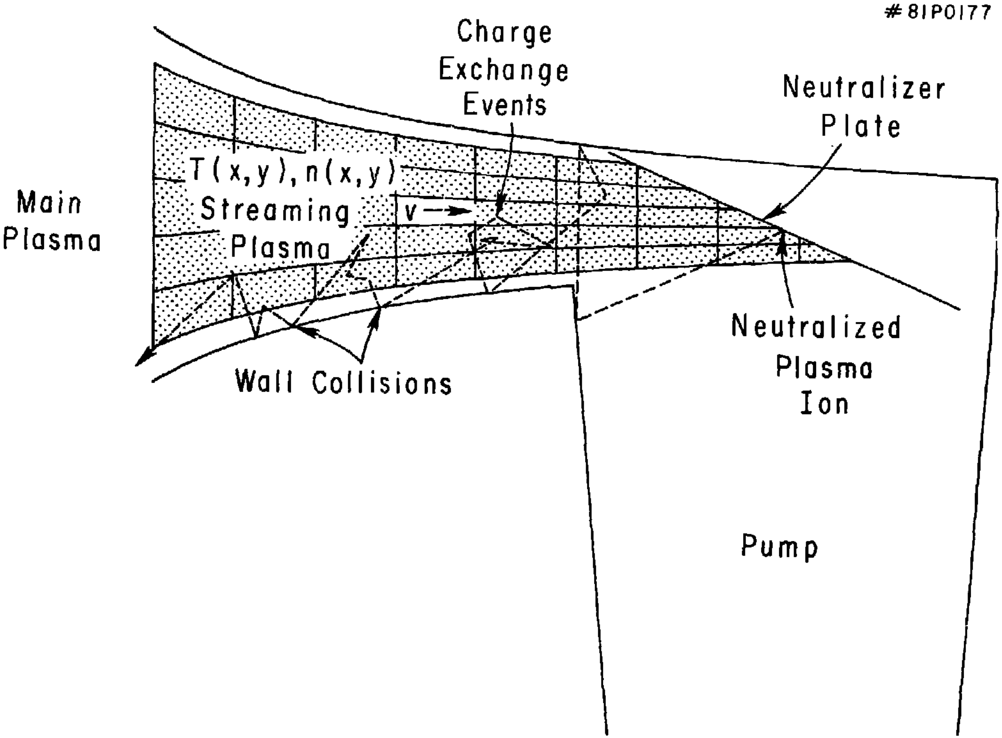
#81P0177
Charge
Exchange
Events
Neutralizer
Plate
Main
Plasma
T(x,y), n(x,y)
Streaming
Plasma
v
Wall Collisions
Neutralized
Plasma
Ion
Pump

FIG. 2

#81P0289

HIGH BETA PLASMA

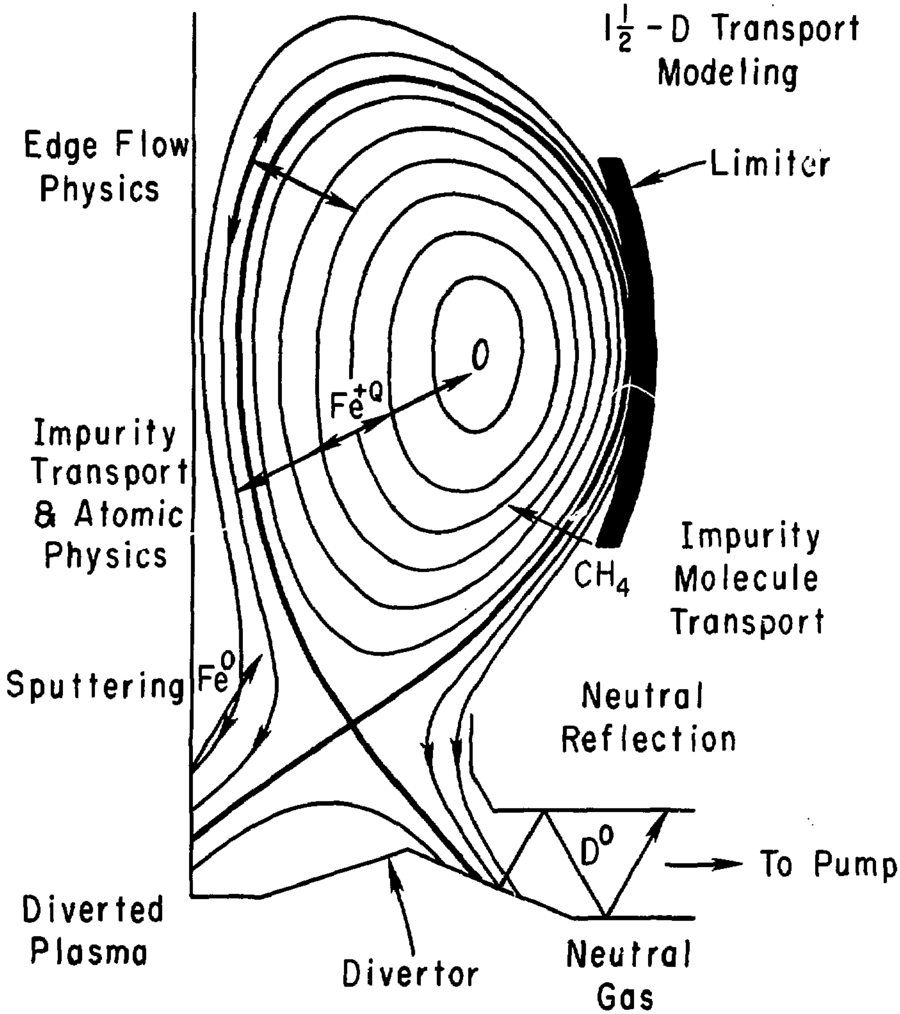

FIG. 3

#82P0052

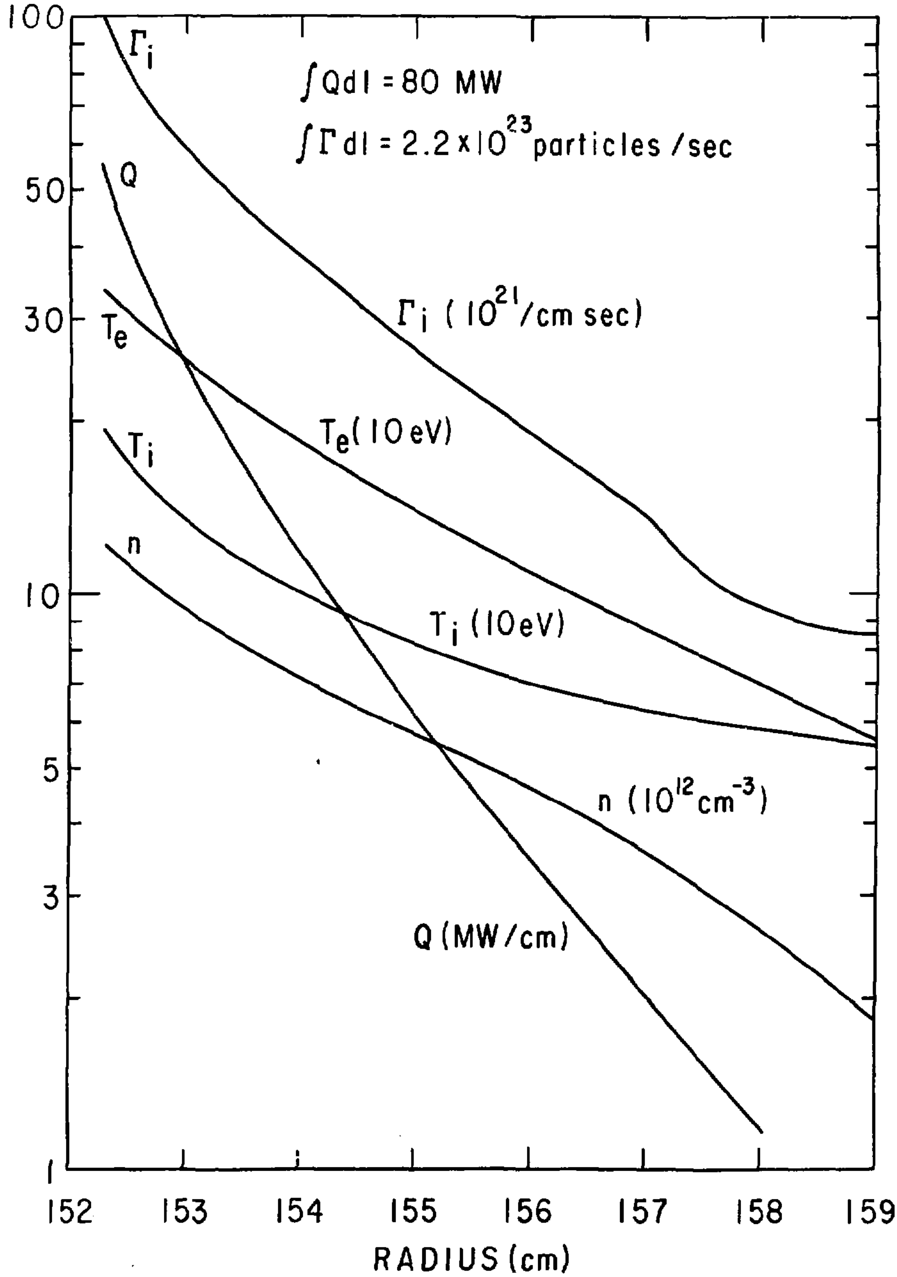

FIG. 4

#82P0082

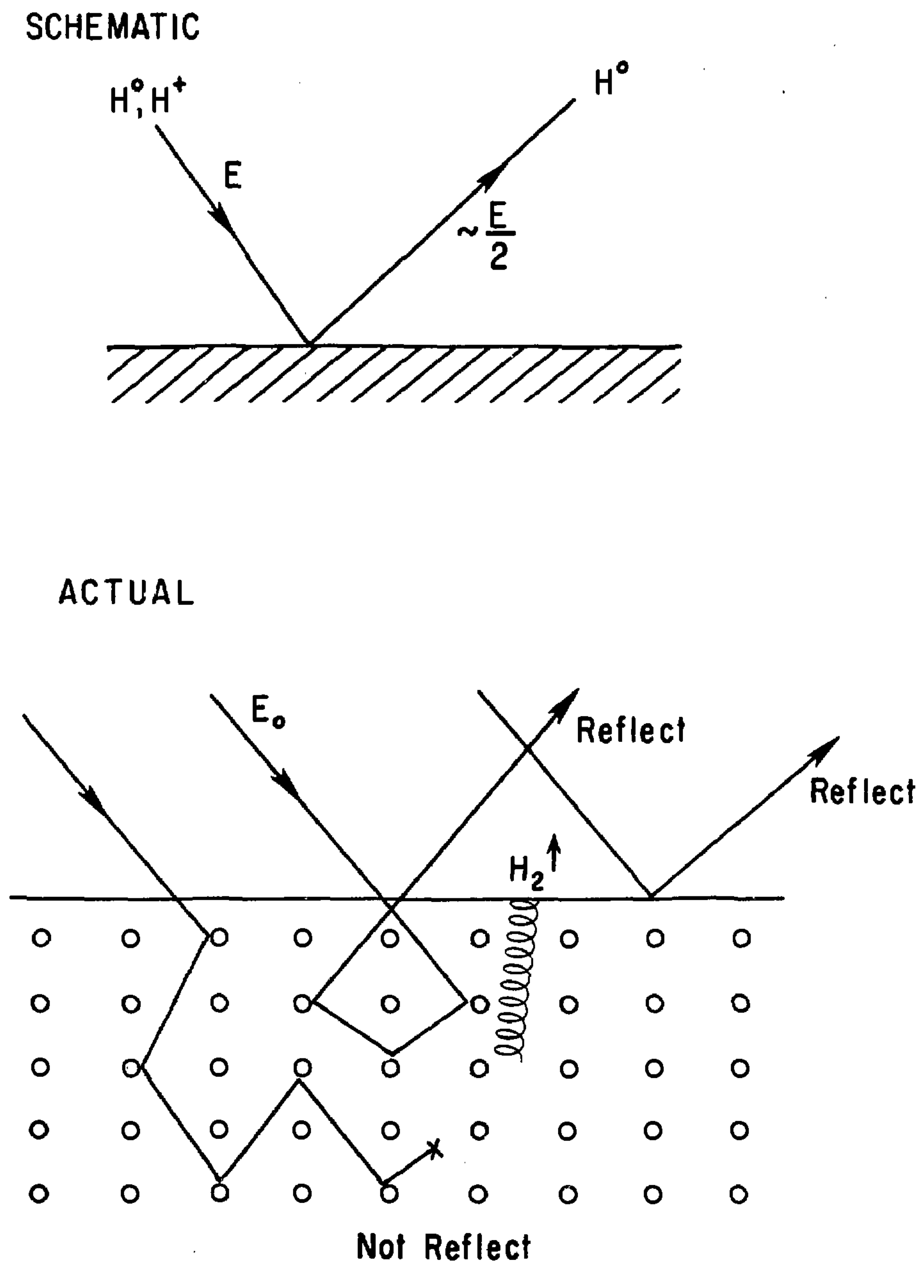

FIG. 5

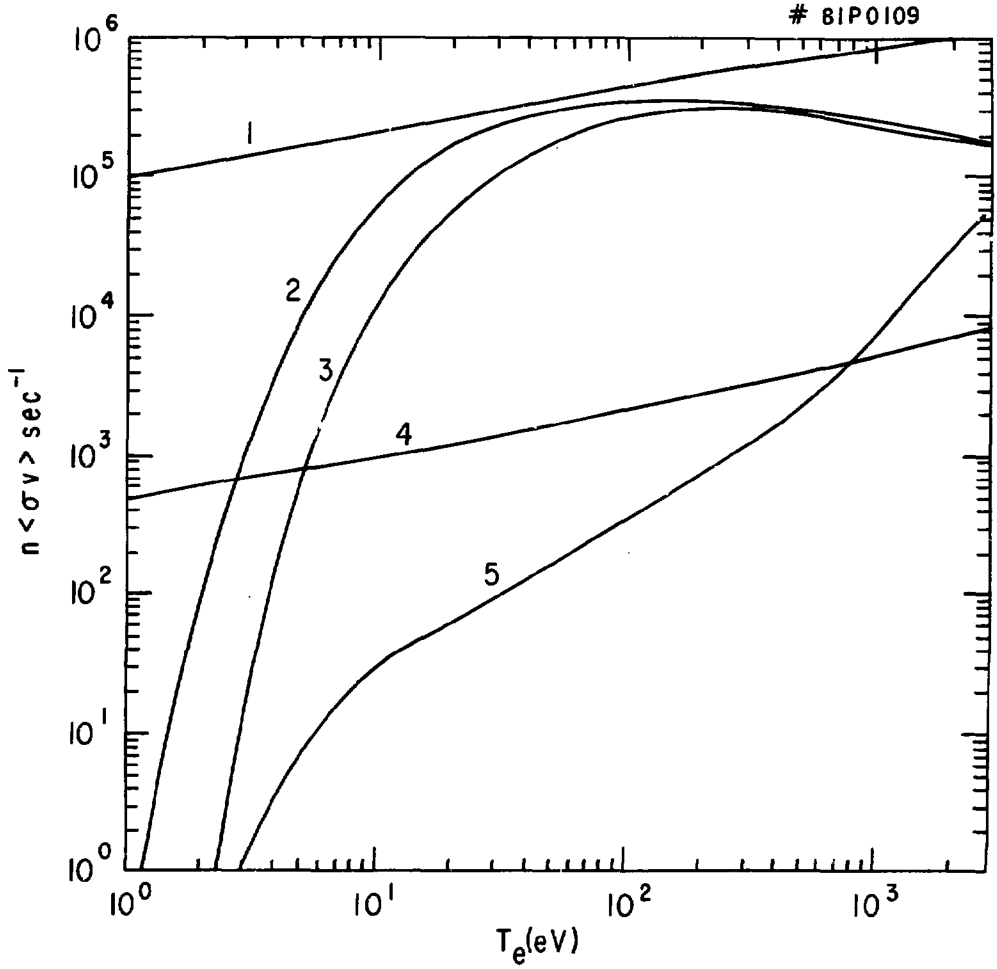

81P0109
10^6
10^5
10^4
10^3
10^2
10^1
10^0
n <σv> sec⁻¹
1
2
3
4
5
10^0
10^1
10^2
10^3
T_e(eV)

FIG. 6a

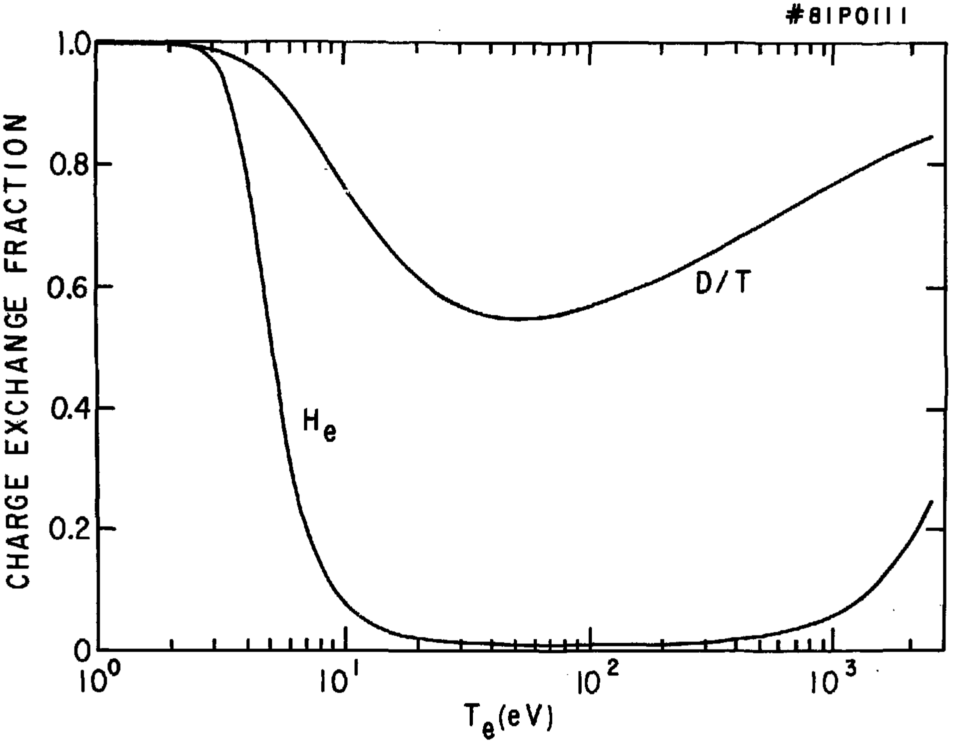
#81P0111
CHARGE EXCHANGE FRACTION
1.0
0.8
0.6
0.4
0.2
0
10^0
10^1
10^2
10^3
T_e(eV)
H_e
D/T

FIG. 6b

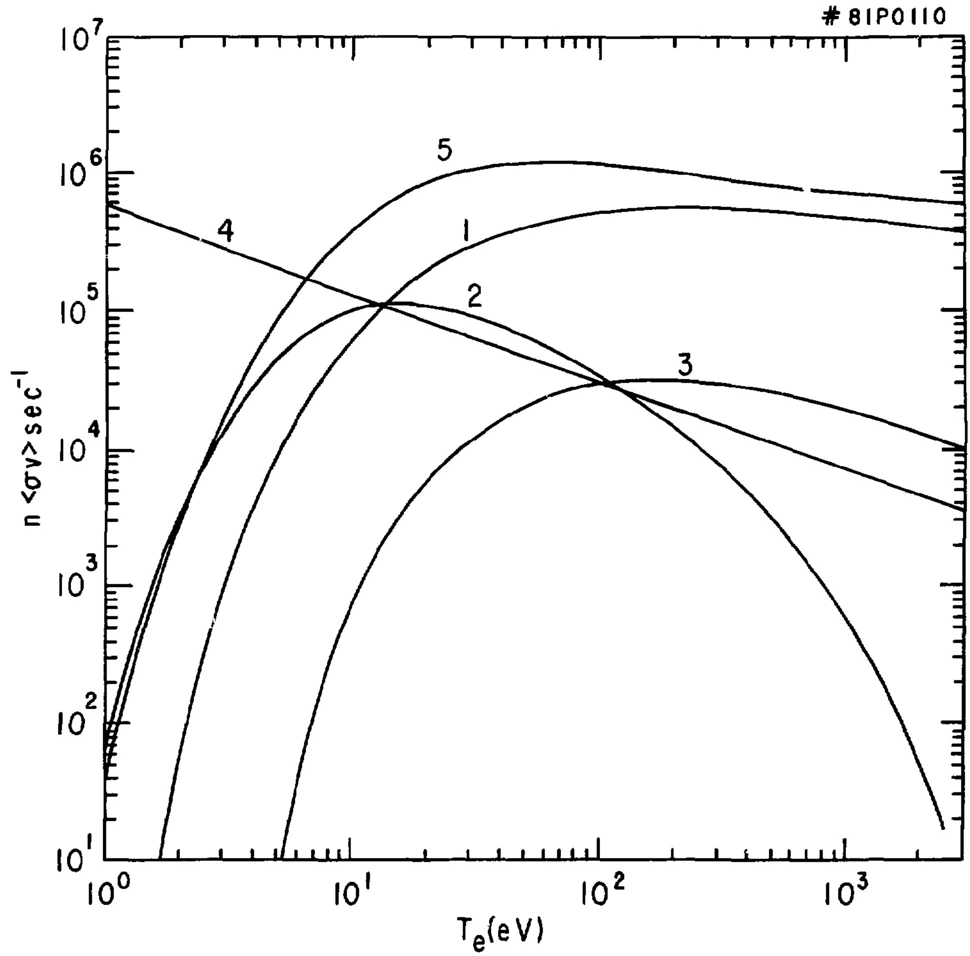

81P0110
10^7
10^6
10^5
10^4
10^3
10^2
10^1
n <σv> sec^{-1}
5
4
1
2
3
10^0
10^1
10^2
10^3
T_e(eV)

FIG. 6c

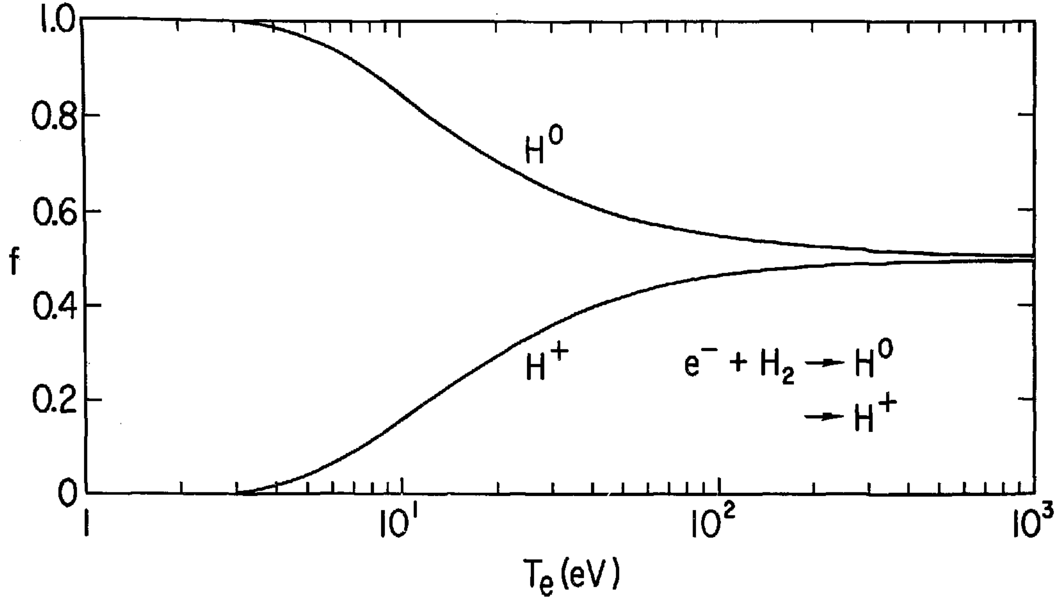
1.0
0.8
0.6
0.4
0.2
0
f
H^0
H^+
$e^- + H_2 \rightarrow H^0$
$\rightarrow H^+$
1
10^1
10^2
10^3
T_e (eV)

FIG. 7

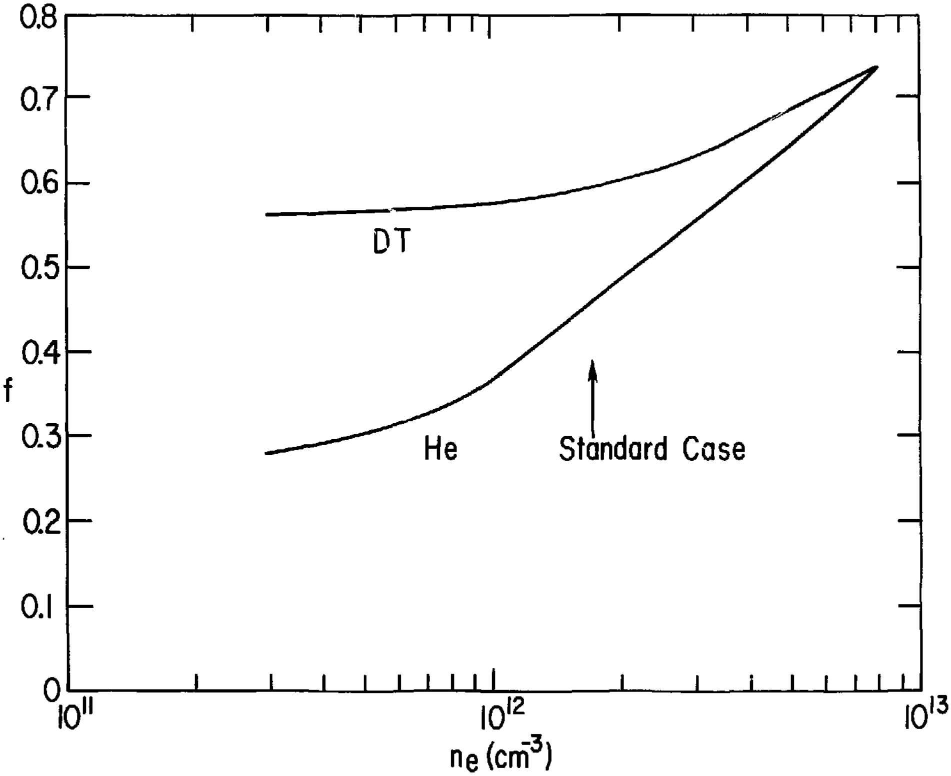
0.8
0.7
0.6
0.5
0.4
0.3
0.2
0.1
0
f
DT
He
Standard Case
10^{11}
10^{12}
10^{13}
n_e (cm^{-3})

FIG. 8

#81P0098

MODEL DIVERTOR CHAMBER

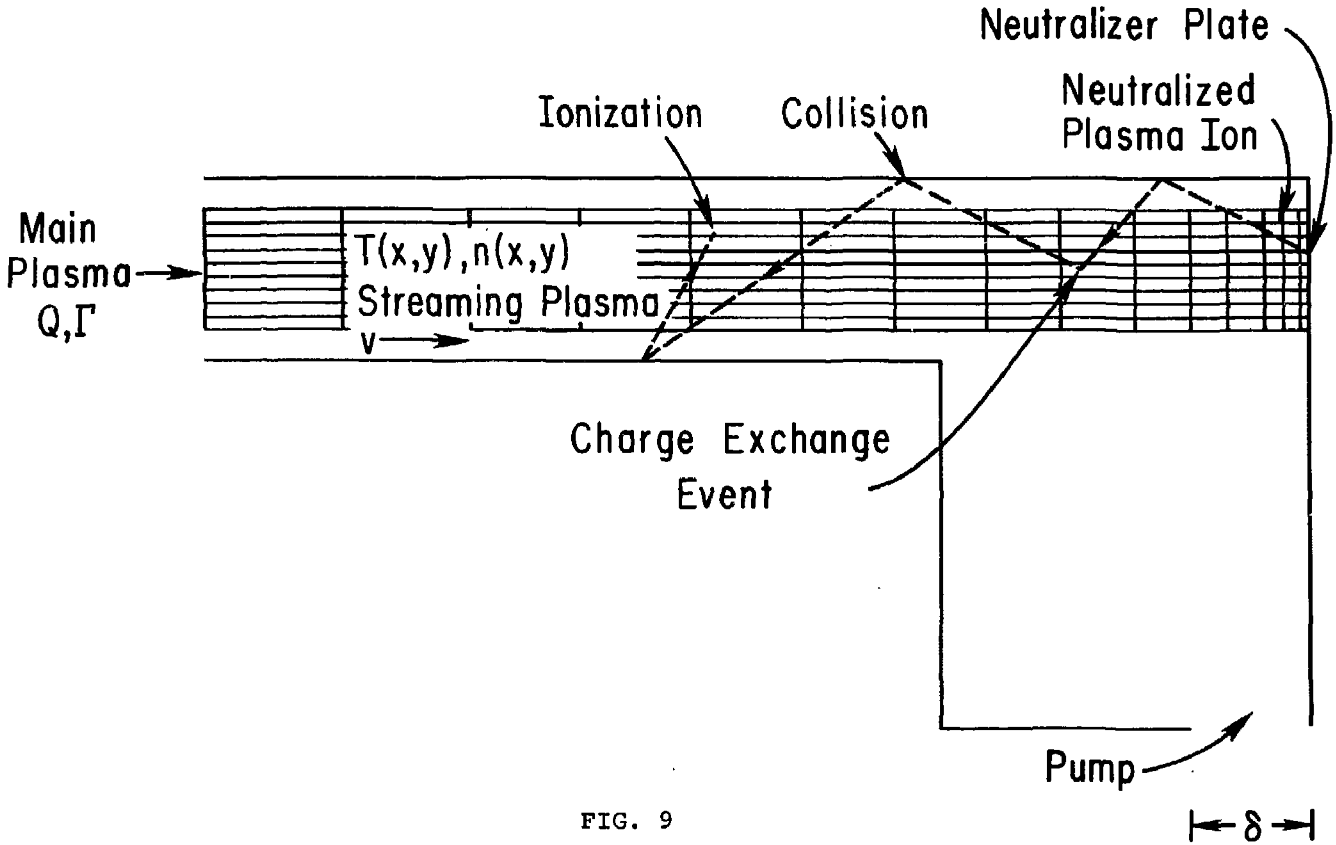

FIG. 9

81P0292

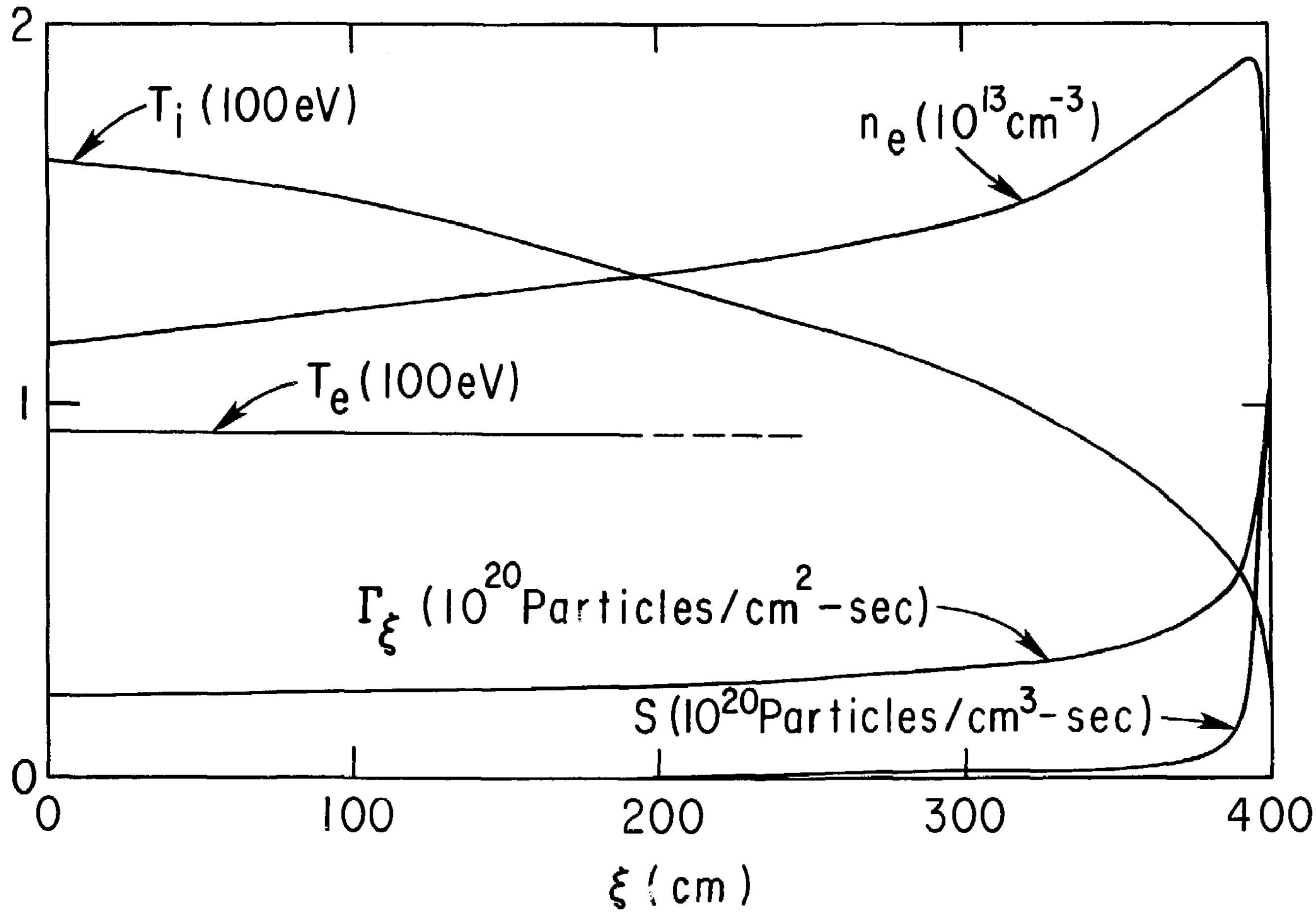

FIG. 10

81P0293

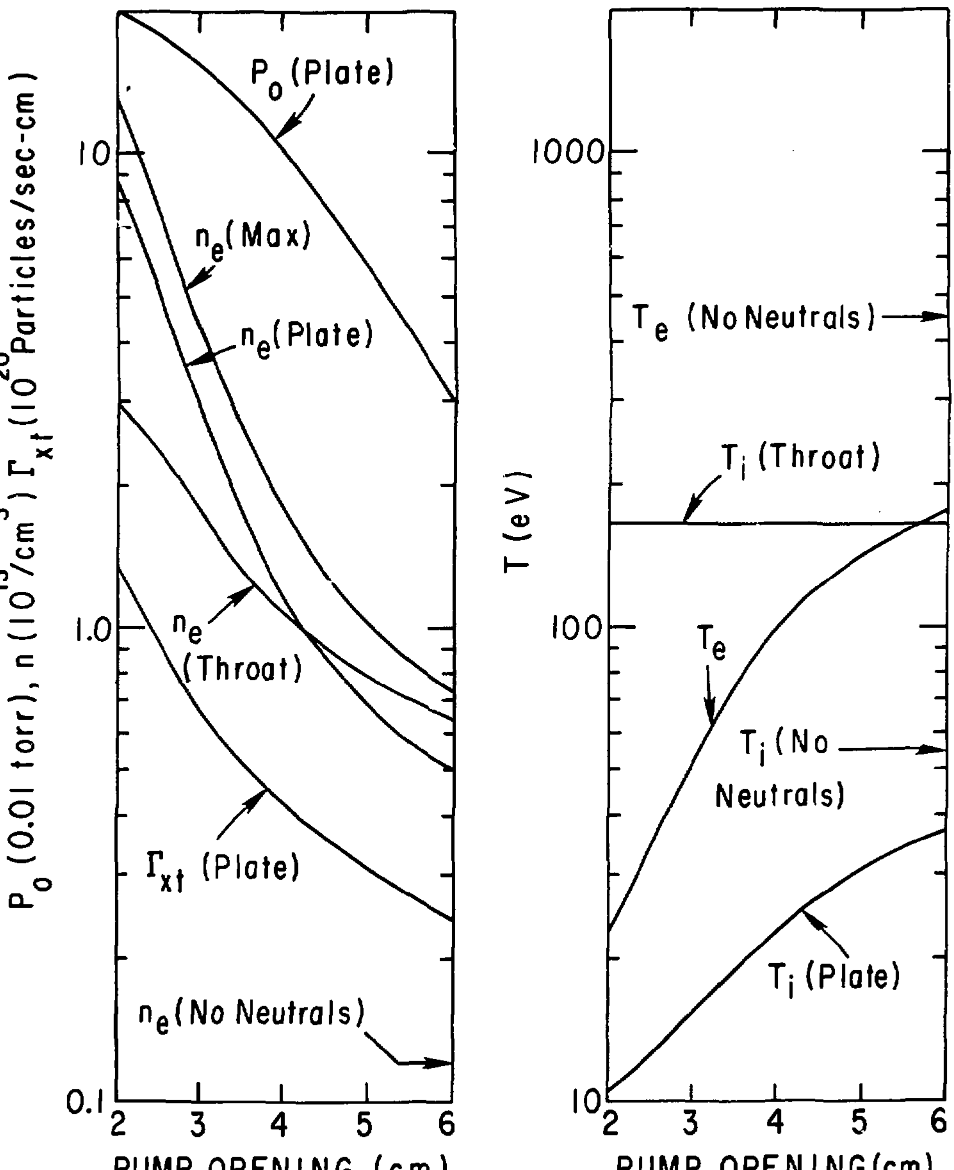

FIG. 11

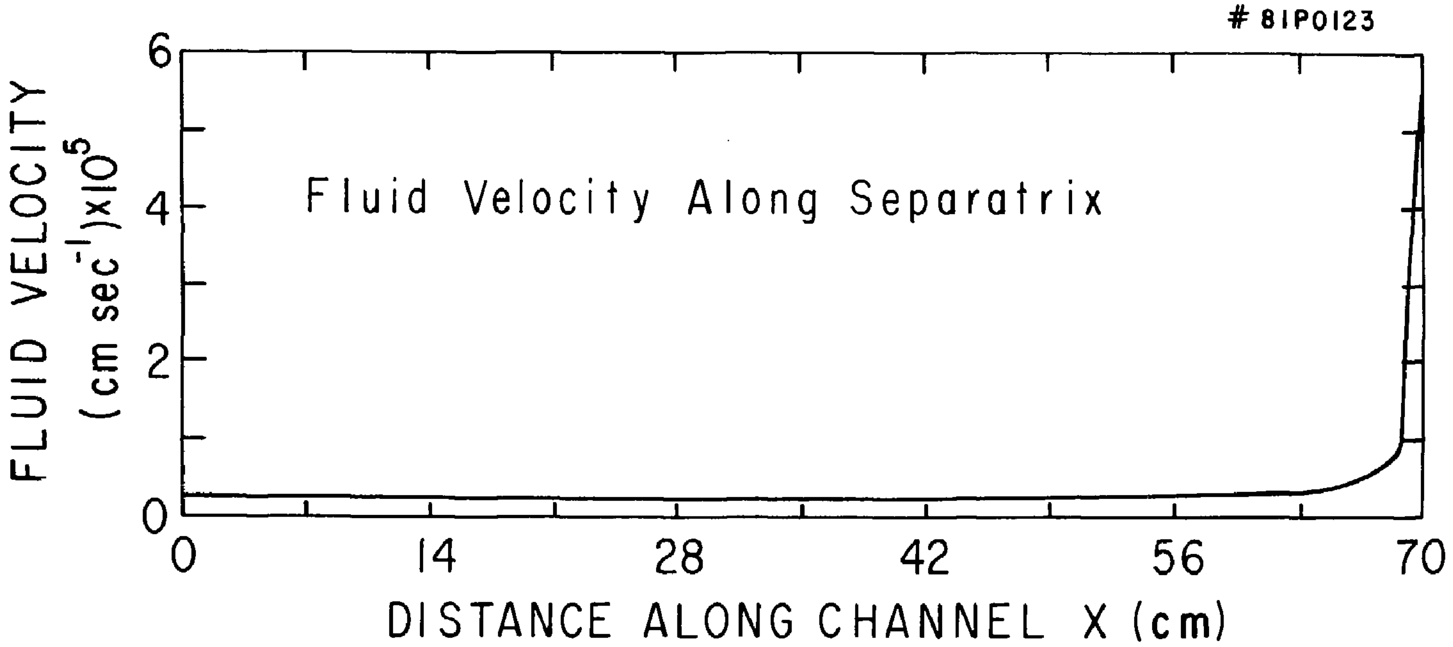

81P0123
FLUID VELOCITY
(cm sec-1)x10^5
6
4
2
0
Fluid Velocity Along Separatrix
0
14
28
42
56
70
DISTANCE ALONG CHANNEL X (cm)

FIG. 12